

A New Approach to Model Updating in Symmetric Structures

Jonathan L. du Bois* and Nick A. J. Lieven†

University of Bristol, Queens Building, University Walk, Bristol, BS8 1TR, England
and Sondipon Adhikari‡

Swansea University, Singleton Park, Swansea SA2 8PP, United Kingdom

Finite element model updating and system identification in symmetric structures is hampered by the inability of the eigenvalues to distinguish between symmetric parameter perturbations. A typical approach is to employ eigenvectors, or even antiresonances, as updating variables. These tend to be less accurate than the eigenvalue measurements however. In this paper, a method for updating symmetric parameters is presented based on quantitative information from the eigenvalues and qualitative information from the eigenvectors. It exploits the effect of eigenvalue curve veering, manifested through modal couplings. The curve veering is measured experimentally by variation of a control parameter. A computationally efficient updating scheme is applied, requiring only a single eigensolution at each iteration. Using experimental data the method is shown to be capable of producing a unique solution to a doubly symmetric updating problem. The ideas presented are expected to prove valuable in localisation problems, stability studies and damage detection.

Nomenclature

Symbols

β	angle between current eigenvector set and datum eigenvector set in the mass-normalised basis
δ_j	system parameter
$\boldsymbol{\varepsilon}_n$	updating variable error vector from n^{th} iteration
κ_{ijk}	modal coupling for i^{th} and k^{th} eigenvalues with respect to parameter δ_j
μ_λ	mean eigenvalue
σ_{iji}	sensitivity of i^{th} eigenvalue to parameter δ_j
$\Delta\lambda_{ki}$	difference in eigenvalues of modes i and k , $\lambda_k - \lambda_i$
$\Delta\sigma_{kji}$	difference in sensitivities of modes k and i to parameter δ_j , $\sigma_{kjk} - \sigma_{iji}$
$\Delta\boldsymbol{\delta}_n$	updating parameter increment vector from n^{th} iteration
Λ_{ik}	diagonal matrix of i^{th} and k^{th} eigenvalues
Ω_{Kik}	i^{th} and k^{th} eigenvector rotation rate in the normal basis with respect to parameter δ_K
Φ_{ik}	matrix of i^{th} and k^{th} mass-normalised eigenvectors
Σ_{ijk}	modal sensitivity matrix for i^{th} and k^{th} modes to parameter δ_j
\mathbf{z}_m	updating variable vector from measured data
\mathbf{z}_n	updating variable vector from n^{th} iteration
\mathbf{K}	stiffness matrix
\mathbf{M}	mass matrix

*Department of Aerospace Engineering, University of Bristol

†Dean, Engineering Faculty, University of Bristol

‡Chair of Aerospace Engineering, School of Engineering, Swansea University

S_n	sensitivity matrix for use in updating scheme
T	rotational transform matrix
$W_{\delta\delta}$	weighting matrix for updating parameters
$W_{\varepsilon\varepsilon}$	weighting matrix for updating variables

I. Introduction

Finite Element (FE) model updating has played an important role in dynamic analyses in recent years. Using experimental results to refine and validate analytical models is an essential step in obtaining an accurate representation of complex systems. The process is somewhat of a black art. The skill lies in determining a physically meaningful model which will respond accurately to subsequent configuration changes, as opposed to a model which simply fits the current results set. The difficulty is compounded in the case of periodic or symmetric structures where common updating methods based on eigenvalues alone are categorically incapable of determining a unique solution. Eigenvectors or antiresonances may be used to facilitate the identification of symmetric parameters but the reliability of these experimentally determined quantities is low compared to that of eigenvalues.

In this paper a new method of system identification is proposed, using quantitative measurements from the eigenvalues in conjunction with qualitative eigenvector observations. The technique involves the deliberate variation of a given control parameter to provide a large experimental data set, and relies on modal interactions or “couplings” to differentiate between symmetric properties. This approach not only provides updating variables that are ideally suited to identifying symmetric parameters but also promises greater accuracy than the current alternatives.

In the next section modal coupling is examined and its relation to frequency veering and localisation is discussed. Further properties are introduced to fully describe the modal interactions. Section III details the methods for extracting these properties from experimental data and section IV sets out the updating scheme. The scheme is applied to a symmetric updating problem in section V. Finally, section VI sums up the successes and failures of the technique with respect to this example before focusing on the implications with regard to its general implementation. Target applications are then identified and briefly discussed.

II. Modal Coupling

Modal coupling is a property associated with frequency veering^{1,2} and vibration localisation.³ It refers to the coupling exhibited by two modes with respect to system parameter perturbations.⁴ An elementary example is that of the coupled spring-mass system of Fig. 1. If the coupling spring stiffness s is zero, there is no physical coupling, and two independent vibration modes exist. Keeping k_1 constant and varying k_2 , a plot of the eigenvalues will show one constant line and the other crossing it where $k_1 = k_2$. When s is increased, the physical coupling increases, and in this specific case that corresponds with an increase in modal coupling. The result is that instead of the two eigenvalue loci crossing, they veer abruptly away from each other as they swap trajectories. This behaviour is shown in Fig. 2. The greater the modal coupling, the larger the separation of the eigenvalues at $k_1 = k_2$. Now, if $k_1 = k_2$ is the nominal symmetric structure, the mode shapes at this point are also symmetric. The greater the discrepancy between k_1 and k_2 and the smaller the coupling s , the more localised the modes become, corresponding to motion of primarily one mass or the other. If s is not large then even small discrepancies between the spring stiffnesses may lead to strong localisation.

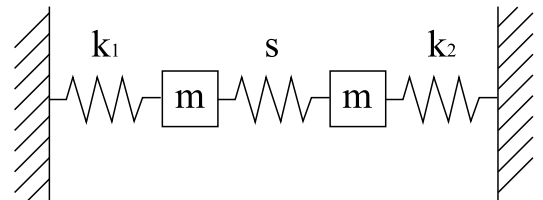


Figure 1. 2-DOF coupled spring-mass system

The localisation is manifested through eigenvector rotations. All the modal properties are swapped in a veering region and for the eigenvectors this takes the form of a continuous rotation through 90° in the normal coordinate system.

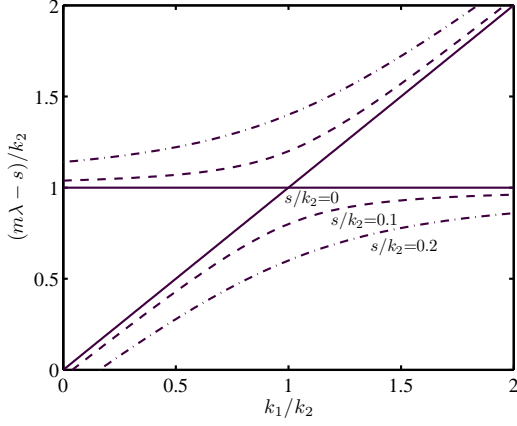


Figure 2. Non-dimensionalised eigenvalue loci, showing veering with respect to variation in the spring stiffnesses as the coupling spring stiffness is increased.

Balmès⁵ demonstrated this behaviour with respect to a simple analytic example, and du Bois *et al.*⁶ derived more general relations for linear mass and stiffness variations. They showed that for proximate modes, the transformations of the eigenvectors can be expressed approximately as a simple rotation within a fixed subspace of the normal basis:

$$\overline{\Phi}_{ik} = \Phi_{ik} \mathbf{T}, \quad \mathbf{T} = \begin{bmatrix} \cos \beta & -\sin \beta \\ \sin \beta & \cos \beta \end{bmatrix} \quad (1)$$

where Φ_{ik} is the mass normalised eigenvector matrix for the i^{th} and k^{th} modes. The midway point in this rotation is referred to as the veering datum, and it is at this point that the eigenvalues are closest, the sensitivities are equal, the curvature is highest and the rate of eigenvector rotation is greatest. The vector set $\overline{\Phi}_{ik}$ will be used to denote this datum set and the overbar will consistently denote properties at the datum.

A “sensitivity matrix” for modes i and k can be defined as

$$\Sigma_{ijk} = \Phi_{ik}^T \frac{d\mathbf{K}}{d\delta_j} \Phi_{ik} - \Phi_{ik}^T \frac{d\mathbf{M}}{d\delta_j} \Phi_{ik} \Lambda_{ik} = \begin{bmatrix} \sigma_{iji} & \kappa_{ijk} \\ \kappa_{kji} & \sigma_{kjk} \end{bmatrix} \quad (2)$$

where \mathbf{M} and \mathbf{K} are the mass and stiffness matrices, Λ_{ik} is a diagonal matrix of the i^{th} and k^{th} eigenvalues, the diagonal terms are the sensitivities of the eigenvalues to parameter δ_j and the off-diagonal terms are the modal coupling responsible for the veering behaviour. The variation of these properties with the vector rotations is described by

$$\sin(2\beta) = \Delta\sigma_{kji}/2\overline{\kappa}_{ijk} \quad (3)$$

$$\cos(2\beta) = \kappa_{ijk}/\overline{\kappa}_{ijk} \quad (4)$$

$$\overline{\kappa}_{ijk}^2 = \kappa_{ijk}^2 + (\Delta\sigma_{kji}/2)^2 \quad (5)$$

where $\Delta\sigma_{kji} = \sigma_{kjk} - \sigma_{iji}$ and $\overline{\kappa}_{ijk}$ is the maximum, or datum, value for the modal coupling. In another paper⁷ the same authors derive expressions for modal properties at the datum: If δ_K is a parameter representing a stiffness variation, the datum parameter value can be found from

$$\overline{\delta}_{Kik} = \delta_K - \frac{\Delta\lambda_{ki}\Delta\sigma_{kKi}}{4\overline{\kappa}_{iKk}^2}. \quad (6)$$

The minimum eigenvalue separation is given by

$$\Delta\overline{\lambda}_{ki} = \frac{\kappa_{iKk}}{\overline{\kappa}_{iKk}} \Delta\lambda_{ki} \quad (7)$$

where $\Delta\lambda_{ki} = \lambda_k - \lambda_i$. The mean eigenvalue at the veering datum is described by

$$\overline{\mu}_{\lambda ik} = \mu_{\lambda ik} - \frac{(\sigma_{iKi} + \sigma_{kKk})\Delta\lambda_{ki}\Delta\sigma_{kKi}}{8\overline{\kappa}_{iKk}^2}. \quad (8)$$

where $\mu_{\lambda} = \frac{\lambda_i + \lambda_k}{2}$. Finally, the maximum eigenvector rotation rate in the normal basis is given by

$$\overline{\Omega}_{Kik} = \frac{d\beta}{d\delta_K} = \frac{\overline{\kappa}_{iKk}}{\Delta\overline{\lambda}_{ki}}. \quad (9)$$

Importantly, all of the datum properties can be calculated from a single eigensolution, obtained anywhere in the vicinity of the veering region.

III. Experimental Parameter Extraction

The focus of these investigations is on using characteristics of the modal interactions as model updating variables. In this section, appropriate quantities are discussed, and methods of experimental determination are described based primarily on the measured eigenvalues.

To fully define the eigenvalue curves in a linear veering region, five quantities are required. For example, one option is to use the gradients and offsets of the nominal (uncoupled) eigenvalue loci along with the eigenvalue separation at the datum. The system adopted here is slightly different, as shown in Fig. 3. The loci are described in terms of the mean eigenvalue gradient, the datum location on the parameter and eigenvalue axes, and the separation and modal coupling at the datum. In fact, from eqn. (5) the datum coupling value is seen to be representative of the difference in gradients of the two uncoupled eigenvalue loci.

The experimental method involves performing modal tests over a range of control parameter values, δ_K . Curve fitting techniques are then applied to all of the eigenvalue datasets in two distinct stages: one to fit the linear mean eigenvalue locus, and a second to determine the nonlinear relationship between the two loci.

The first stage is straightforward to implement: for each dataset the mean eigenvalue, μ_λ , is calculated and the least squares linear fit is obtained using

$$\begin{Bmatrix} p_1 \\ p_2 \end{Bmatrix} = \begin{bmatrix} \delta_K^{(1)} & 1 \\ \delta_K^{(2)} & 1 \\ \vdots & \vdots \\ \delta_K^{(n)} & 1 \end{bmatrix}^+ \begin{Bmatrix} \mu_\lambda^{(1)} \\ \mu_\lambda^{(2)} \\ \vdots \\ \mu_\lambda^{(n)} \end{Bmatrix} \quad (10)$$

where bracketed superscripts denote the experimental dataset and + denotes the pseudo-inverse such that

$$\mathbf{A}^+ = (\mathbf{A}^T \mathbf{A})^{-1} \mathbf{A}^T. \quad (11)$$

The gradient of the line and the mean eigenvalue at the veering datum are given by

$$\frac{d\mu_\lambda}{d\delta_K} = p_1 \quad \text{and} \quad \bar{\mu}_\lambda = \bar{\delta}_K p_1 + p_2. \quad (12)$$

The second stage relates the two loci in terms of the eigenvalue separation, $\Delta\lambda_{ki}$. From eqns. (5), (6) and (7),

$$\Delta\lambda_{ki}^2 = (4\bar{\kappa}_{iKk}^2)\delta_K^2 - (8\bar{\kappa}_{iKk}^2\bar{\delta}_{Kik})\delta_K + (4\bar{\kappa}_{iKk}^2\bar{\delta}_{ik}K^2 + \Delta\bar{\lambda}_{ki}^2). \quad (13)$$

Thus in the vicinity of the veering, $\Delta\lambda_{ki}^2$ is described by a quadratic in the control parameter δ_K . The least squares curve fit is obtained from

$$\mathbf{q} = \begin{bmatrix} \delta_K^{(1)2} & \delta_K^{(1)} & 1 \\ \delta_K^{(2)2} & \delta_K^{(2)} & 1 \\ \vdots & \vdots & \vdots \\ \delta_K^{(n)2} & \delta_K^{(n)} & 1 \end{bmatrix}^+ \begin{Bmatrix} \Delta\lambda_{ki}^{(1)2} \\ \Delta\lambda_{ki}^{(2)2} \\ \vdots \\ \Delta\lambda_{ki}^{(n)2} \end{Bmatrix} \quad (14)$$

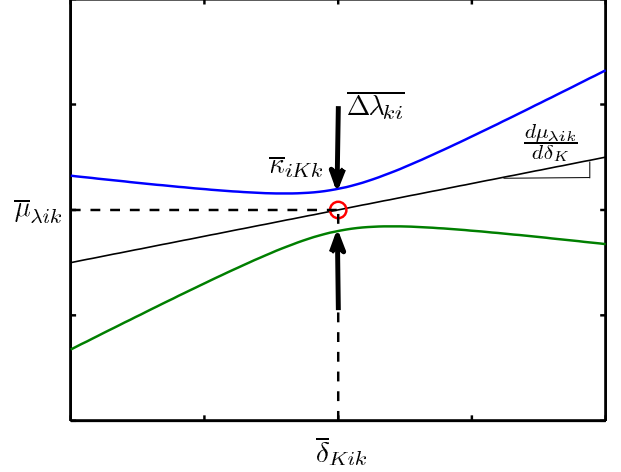


Figure 3. Modal characteristics used to define veering eigenvalue curves.

where

$$\mathbf{q} = \left\{ \begin{array}{c} 4\bar{\kappa}_{iKk}^2 \\ -8\bar{\kappa}_{iKk}^2 \bar{\delta}_{Kik} \\ 4\bar{\kappa}_{iKk}^2 \bar{\delta}_{Kik}^2 + \Delta\bar{\lambda}_{ki}^2 \end{array} \right\}. \quad (15)$$

From eqn. (15) the veering properties $|\bar{\kappa}_{iKk}|$, $\bar{\delta}_{Kik}$ and $\Delta\bar{\lambda}_{ki}$ may be established in turn, and all that remains is to determine the sign of $\bar{\kappa}_{iKk}$. This is not possible from consideration of the eigenvalues alone, and the eigenvectors must be consulted. First a set of reference vectors should be established to be used with both the analytic and empirical data. The measured eigenvector orientations can be determined relative to the reference vectors using scalar (dot) products. Their rotation should be plotted as a smooth curve, and from eqn. (9), positive modal coupling corresponds with positive $d\beta/d\delta_K$ (and hence negative vector rotation direction as β is the angle *from* Φ_{ik} to $\bar{\Phi}_{ik}$). It is this distinction in sign that allows the determination of parameters which would otherwise be insoluble due to symmetry.

IV. Model Updating

A sensitivity-based updating scheme is employed here, as described by Friswell and Mottershead.⁸ The variation of the eigenvalues with respect to the control parameter is used to compute the updating variables. These in turn are used to identify values for the updating parameters. This section will first describe the updating scheme before discussing the choice of updating variables.

The basis for this method lies in the linearisation of the updating variable sensitivities about the current updating parameter values for each iteration. These sensitivities are then used to determine the parameter values that minimise the least squares error in the updating variables. If the updating variables computed from the measured data are represented by the vector \mathbf{z}_m , and those computed in the n^{th} analytic iteration are contained in \mathbf{z}_n , then the updating variable error vector is

$$\boldsymbol{\varepsilon}_n = \mathbf{z}_m - \mathbf{z}_n. \quad (16)$$

The change in parameter values at iteration n is given by

$$\Delta\boldsymbol{\delta}_n = [\mathbf{S}_n^T \mathbf{W}_{\varepsilon\varepsilon} \mathbf{S}_n + \mathbf{W}_{\delta\delta}]^{-1} \mathbf{S}_n^T \mathbf{W}_{\varepsilon\varepsilon} \boldsymbol{\varepsilon}_n \quad (17)$$

where \mathbf{S}_n is the updating variable sensitivity matrix and $\mathbf{W}_{\varepsilon\varepsilon}$ and $\mathbf{W}_{\delta\delta}$ are weighting matrices for the updating variables and parameters, respectively.

The sensitivities are computed from the analytic model. du Bois *et al.*⁹ derive the sensitivities of the properties discussed in section II with respect to an updating parameter δ_p (distinct from the control parameter δ_K). The first step is to obtain the derivative of the eigenvalue sensitivities and modal coupling, contained within the sensitivity matrix. Differentiating eqn. (2) with respect to an arbitrary parameter δ_p and remembering $\frac{d\mathbf{M}}{d\delta_K} = 0$ produces

$$\frac{d\boldsymbol{\Sigma}_{iKk}}{d\delta_p} = \left[\begin{array}{cc} \frac{d\sigma_{iKk}}{d\delta_p} & \frac{d\kappa_{iKk}}{d\delta_p} \\ \frac{d\kappa_{kKk}}{d\delta_p} & \frac{d\sigma_{kKk}}{d\delta_p} \end{array} \right] = \frac{d\Phi_{ik}}{d\delta_p}^T \frac{d\mathbf{K}}{d\delta_K} \Phi_{ik} + \Phi_{ik}^T \frac{d\mathbf{K}}{d\delta_K} \frac{d\Phi_{ik}}{d\delta_p}, \quad (18)$$

where the parameters δ_K and δ_p are assumed to be independent so that $\frac{d^2\mathbf{K}}{d\delta_K d\delta_p} = 0$. The tangent stiffness derivative $\frac{d\mathbf{K}}{d\delta_K}$ is determined using a numerical finite difference technique:

$$\frac{d\mathbf{K}}{d\delta_K} = \frac{\mathbf{K}^{(z+1)} - \mathbf{K}^{(z)}}{\delta_K^{(z+1)} - \delta_K^{(z)}} \quad (19)$$

where the bracketed superscripts in this case refer to the parameter increment. The eigenvalue derivative $\frac{d\Phi_{ik}}{d\delta_p}$ is best obtained with Nelson's method,¹⁰ the eigenvalue derivatives are obtained with Fox and Kapoor's equation,¹¹ and the following relationships are noted:

$$\frac{d\Delta\lambda_{ki}}{d\delta_p} = \frac{d\lambda_k}{d\delta_p} - \frac{d\lambda_i}{d\delta_p} \quad \frac{d\Delta\sigma_{ki}}{d\delta_p} = \frac{d\sigma_k}{d\delta_p} - \frac{d\sigma_i}{d\delta_p}. \quad (20)$$

The sensitivity of the maximum modal coupling is determined by differentiating eqn. (5) to produce

$$\frac{d}{d\delta_p} \bar{\kappa}_{iKk}^2 = 2\kappa_{iKk} \frac{d\kappa_{iKk}}{d\delta_p} + \frac{\Delta\sigma_{ki}}{2} \frac{d\Delta\sigma_{ki}}{d\delta_p} \quad (21)$$

and hence

$$\frac{d}{d\delta_p} \bar{\kappa}_{iKk} = \frac{\kappa_{iKk}}{\bar{\kappa}_{iKk}} \frac{d\kappa_{iKk}}{d\delta_p} + \frac{\Delta\sigma_{ki}}{4\bar{\kappa}_{iKk}} \frac{d\Delta\sigma_{ki}}{d\delta_p}. \quad (22)$$

The sensitivity of the minimum eigenvalue separation is found by differentiating eqn. (7), yielding

$$\frac{d\Delta\bar{\lambda}_{ki}}{d\delta_p} = \frac{\kappa_{iKk}}{\bar{\kappa}_{iKk}} \frac{d\Delta\lambda_{ki}}{d\delta_p} + \frac{\Delta\lambda_{ki}}{\bar{\kappa}_{iKk}} \frac{d\kappa_{iKk}}{d\delta_p} - \frac{\Delta\lambda_{ki}\kappa_{iKk}}{\bar{\kappa}_{iKk}^2} \frac{d\bar{\kappa}_{iKk}}{d\delta_p}. \quad (23)$$

It is now possible to determine the derivative of the maximum vector rotation rate from eqn. (9). Noting that $\bar{\Omega}_{Kik}^{-1}$ is discontinuous across $\Delta\lambda_{ki} = 0$, however, the preferred quantity for the purposes of updating is its inverse, whose sensitivity is

$$\frac{\partial\bar{\Omega}_{Kik}^{-1}}{\partial\delta_p} = \frac{1}{\bar{\kappa}_{iKk}} \frac{d\Delta\bar{\lambda}_{ki}}{d\delta_p} - \frac{\Delta\bar{\lambda}_{ki}}{\bar{\kappa}_{iKk}^2} \frac{d\bar{\kappa}_{iKk}}{d\delta_p}. \quad (24)$$

Similarly the derivative of the datum parameter value is found by rearranging and differentiating eqn. (6) to give

$$\frac{d\bar{\delta}_{Kik}}{d\delta_p} = \frac{\Delta\sigma_{ki}\Delta\lambda_{ki}}{4\bar{\kappa}_{iKk}^4} \frac{\partial}{\partial\delta_p} \bar{\kappa}_{iKk}^2 - \frac{\Delta\sigma_{ki}}{4\bar{\kappa}_{iKk}^2} \frac{d\Delta\lambda_{ki}}{d\delta_p} - \frac{\Delta\lambda_{ki}}{4\bar{\kappa}_{iKk}^2} \frac{d\Delta\sigma_{ki}}{d\delta_p}. \quad (25)$$

Finally, eqn. (8) is differentiated to give

$$\begin{aligned} \frac{d\bar{\mu}_\lambda}{d\delta_p} &= \frac{1}{2} \left(\frac{d\lambda_i}{d\delta_p} + \frac{d\lambda_k}{d\delta_p} \right) - \frac{\Delta\lambda_{ki}\Delta\sigma_{ki}}{8\bar{\kappa}_{iKk}^2} \left(\frac{d\sigma_i}{d\delta_p} + \frac{d\sigma_k}{d\delta_p} \right) \\ &\quad - \frac{(\sigma_i + \sigma_k)\Delta\sigma_{ki}}{8\bar{\kappa}_{iKk}^2} \frac{d\Delta\lambda_{ki}}{d\delta_p} - \frac{(\sigma_i + \sigma_k)\Delta\lambda_{ki}}{8\bar{\kappa}_{iKk}^2} \frac{d\Delta\sigma_{ki}}{d\delta_p} \\ &\quad + \frac{(\sigma_i + \sigma_k)\Delta\lambda_{ki}\Delta\sigma_{ki}}{8\bar{\kappa}_{iKk}^4} \frac{d}{d\delta_p} \bar{\kappa}_{iKk}^2. \end{aligned} \quad (26)$$

Once again, these calculations may be performed using the modal results from a single eigensolution, determined anywhere in the region of the veering datum, making the scheme computationally efficient.

In this study the updating is based purely on veering characteristics; in general it is expected that these characteristics will be applied in tandem with other variables such as the eigenvalues themselves. The properties that are selected here, however, are limited to the datum control parameter value and mean eigenvalue (effectively locating the centre of the veering region in Fig. 3), and the maximum vector rotation rate. The latter is chosen as it characterises the extent of the modal coupling while retaining the critical sign information. (In contrast, the modal coupling itself conveys the sign but does not contain the valuable quantitative information, while the minimum eigenvalue separation alone conveys the magnitude but not the sign.)

The sensitivities are assembled into a sensitivity matrix, for example three parameters, δ_p , δ_q and δ_r , could be updated using

$$\mathbf{S}_n = \begin{bmatrix} \frac{\partial}{\partial\delta_p} \bar{\Omega}^{-1} & \frac{\partial}{\partial\delta_q} \bar{\Omega}^{-1} & \frac{\partial}{\partial\delta_r} \bar{\Omega}^{-1} \\ \frac{\partial}{\partial\delta_p} \bar{\delta}_K & \frac{\partial}{\partial\delta_q} \bar{\delta}_K & \frac{\partial}{\partial\delta_r} \bar{\delta}_K \\ \frac{\partial}{\partial\delta_p} \bar{\mu}_\lambda & \frac{\partial}{\partial\delta_q} \bar{\mu}_\lambda & \frac{\partial}{\partial\delta_r} \bar{\mu}_\lambda \end{bmatrix}. \quad (27)$$

An important consideration is the condition number of the sensitivity matrix. Unique updating solutions are reliant on a well conditioned inversion process for this matrix, and in the case of symmetric parameters it is the sign information in the eigenvector rotation rate that contributes to the linear independence of the rows and columns, thus rendering the problem tractable.

V. Application of Methods: Welded Frame Example

The example considered here is an extension of that tackled in a previous presentation by du Bois *et al.*⁷ Where that paper concentrated on the theoretical derivations, this exposition develops a better physical understanding of the problem.

The experimental rig takes the form of a cross-braced rectangle, seen in Fig. 4. Two bolts in one of the cross-members allow tensioning of the structure which induces stress-stiffening, a geometric nonlinearity whereby the transverse stiffness of slender elements is affected by axial loading. A detailed description of the analytical model, experimental setup and results can be found in earlier publications.^{2,7,12}

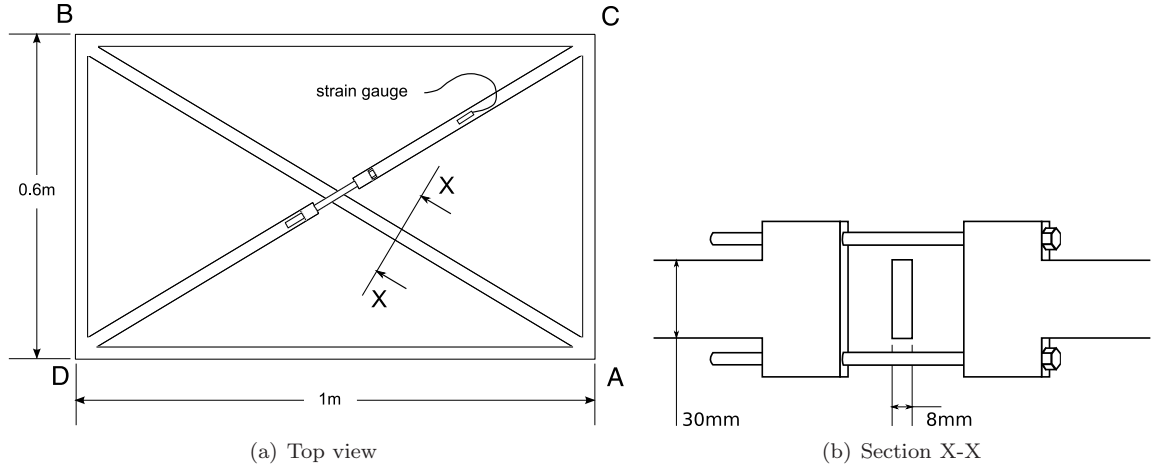


Figure 4. Cross-braced rectangular frame used for updating tests.

The uncertainty in this structure lies in the weld stiffnesses in the corners. There are twelve joints (three members meeting in each of four corners), but to simplify the study only four will be considered: those between the diagonal members and the rest of the frame in each corner. The remaining joint stiffnesses will be accounted for very crudely by a global Young's modulus factor. The parameters are denoted δ_A , δ_B , δ_C , δ_D and δ_E , corresponding to the corner joint labels in Fig. 4 and the Young's modulus factor, respectively. The joint stiffness parameters define the width of short beam elements included at the ends of the diagonal members, as a fraction of the beams' full thickness. The difficulty posed by this problem is that of obtaining a unique solution for the four symmetric parameters δ_{A-D} .

As the structure is loaded, several of the natural frequency loci form intersections. The intersections of interest are those where a symmetric and an antisymmetric mode meet. It has been noted¹³ that such modes will cross in a perfectly symmetric structure but will veer in the presence of imperfections. It is these veerings that will allow parameters δ_{A-D} to be determined authoritatively. The fifth parameter, δ_E , is included to allow better convergence of the solution and to give an indication of the influence of the remaining eight unmodelled joint stiffnesses.

The experimental data presents two suitable veering regions, covering the two reflective symmetry planes in the structure. These are for mode pairs 2-3 and 5-6. The remaining rotational symmetry cannot be resolved by the available data so the updating problem is recast in terms of the the average stiffness and the stiffness differences about the reflective symmetry planes:

$$\delta_M = \frac{1}{4} \sum_{a=A}^D \delta_a \quad \begin{aligned} \delta_X &= \delta_B - \delta_C = \delta_D - \delta_A \\ \delta_Y &= \delta_D - \delta_B = \delta_A - \delta_C \end{aligned} \quad (28)$$

The full sensitivity matrix now becomes

$$\mathbf{S} = \begin{bmatrix} \frac{\partial}{\partial \delta_M} \bar{\Omega}_{K23}^{-1} & \frac{\partial}{\partial \delta_X} \bar{\Omega}_{K23}^{-1} & \frac{\partial}{\partial \delta_Y} \bar{\Omega}_{K23}^{-1} & \frac{\partial}{\partial \delta_E} \bar{\Omega}_{K23}^{-1} \\ \frac{\partial}{\partial \delta_M} \bar{\delta}_{K23} & \frac{\partial}{\partial \delta_X} \bar{\delta}_{K23} & \frac{\partial}{\partial \delta_Y} \bar{\delta}_{K23} & \frac{\partial}{\partial \delta_E} \bar{\delta}_{K23} \\ \frac{\partial}{\partial \delta_M} \bar{\mu}_{\lambda 23} & \frac{\partial}{\partial \delta_X} \bar{\mu}_{\lambda 23} & \frac{\partial}{\partial \delta_Y} \bar{\mu}_{\lambda 23} & \frac{\partial}{\partial \delta_E} \bar{\mu}_{\lambda 23} \\ \frac{\partial}{\partial \delta_M} \bar{\Omega}_{K56}^{-1} & \frac{\partial}{\partial \delta_X} \bar{\Omega}_{K56}^{-1} & \frac{\partial}{\partial \delta_Y} \bar{\Omega}_{K56}^{-1} & \frac{\partial}{\partial \delta_E} \bar{\Omega}_{K56}^{-1} \\ \frac{\partial}{\partial \delta_M} \bar{\delta}_{K56} & \frac{\partial}{\partial \delta_X} \bar{\delta}_{K56} & \frac{\partial}{\partial \delta_Y} \bar{\delta}_{K56} & \frac{\partial}{\partial \delta_E} \bar{\delta}_{K56} \\ \frac{\partial}{\partial \delta_M} \bar{\mu}_{\lambda 56} & \frac{\partial}{\partial \delta_X} \bar{\mu}_{\lambda 56} & \frac{\partial}{\partial \delta_Y} \bar{\mu}_{\lambda 56} & \frac{\partial}{\partial \delta_E} \bar{\mu}_{\lambda 56} \end{bmatrix}. \quad (29)$$

Only four updating variables are required to update the four parameters, two of which must be $\bar{\Omega}_{K23}^{-1}$ and $\bar{\Omega}_{K56}^{-1}$. Ordinarily the best approach would be to select the combination which produces the best conditioning for the problem. For illustrative purposes, however, this update will seek to reproduce the veering behaviour of modes 5 and 6, so $\bar{\delta}_{K56}$ and $\bar{\mu}_{\lambda 56}$ are chosen for the remaining two. The condition number for the resulting sensitivity matrix is 448, which is satisfactory.

The squared eigenvalue separation from the experimental data is plotted for both mode pairs in Fig. 5. The quadratic trend is clear in both, although almost half of the parabola is cut off at the left edge of Fig. 5(a), and there is a strong nonlinearity at the higher loading values. It is also apparent that the mild nonlinearity in Fig. 5(b) causes a shift over the course of the loading range. These observations demand careful consideration of the data points used in the curve fitting. Although the nonlinearities suggest that the analysis should be limited to the vicinity of the veering, this requirement is countered by the need to include sufficient points to produce a reliable estimate of the curve.

Figs. 6 and 7 show the variation of the modal properties for both mode pairs as the load range is expanded from the datum to encompass more data points. The most striking feature of the two result sets is that the variation in the property estimates is generally far higher for mode pair 2-3. The conclusion that can be drawn from this finding is that it is important to include both sides of the parabola in the experimental data. This will not only help to average out load-wise nonlinear trends, but will also tend to produce more accurate estimates of the parabola offset from the x-axis, and in turn the minimum eigenvalue separation. Supporting these hypotheses, it is found that in Fig. 7 most of the estimates settle to reasonable values between the 1000N and 3000N ranges before diverging to the invalid global least squares fit. In contrast, Fig. 6 shows underlying downward trends in three of the graphs, as well as a more erratic eigenvalue separation estimate. Subjective estimates of the properties are made, shown as dashed lines in the figures. It is noted that in particular, the eigenvalue separation estimates have a low confidence attached to them. This is attributed primarily to the low accuracy of the load measurements, which could only be made to within approximately 50N.

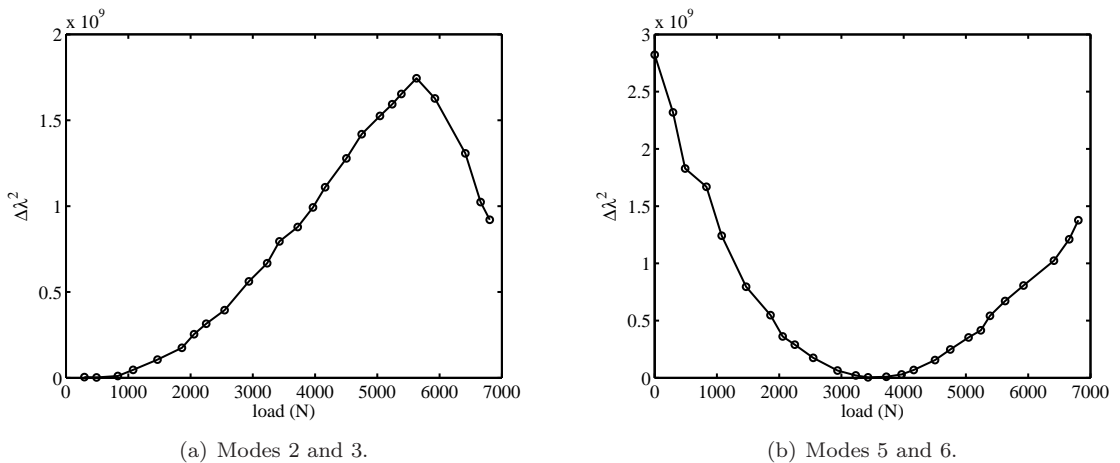
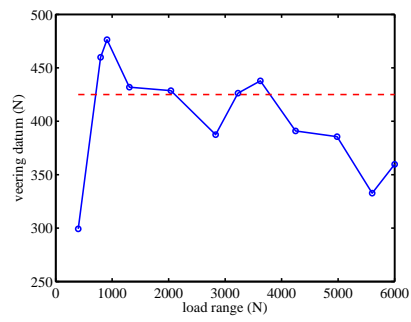
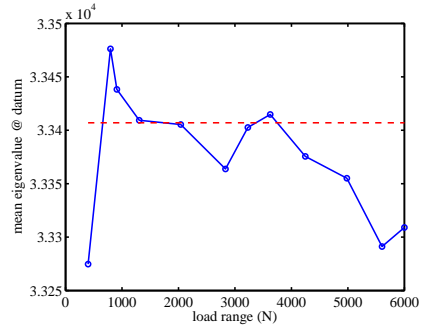


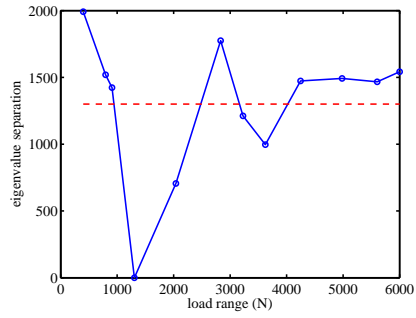
Figure 5. Experimentally determined eigenvalue separation in the welded frame.



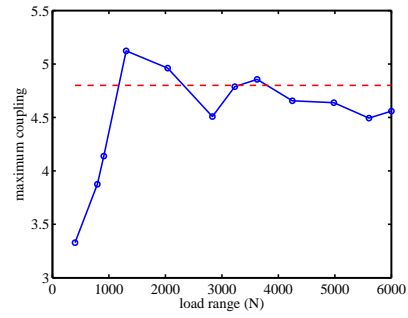
(a) Veering Parameter Datum



(b) Mean Eigenvalue at Datum

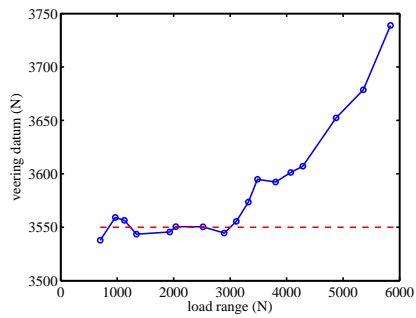


(c) Minimum Eigenvalue Separation

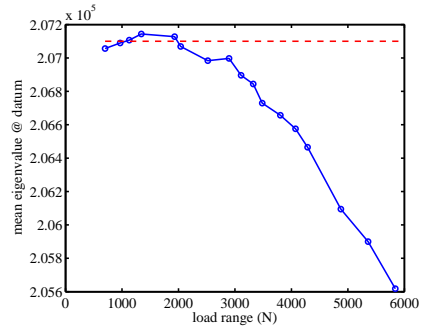


(d) Maximum Modal Coupling

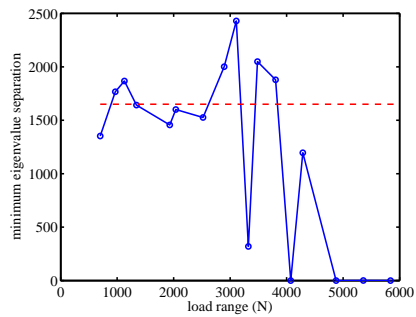
Figure 6. Veering properties extracted from the experimental data using data points from varying load ranges, centered approximately about the veering datum. (Modes 2 and 3.)



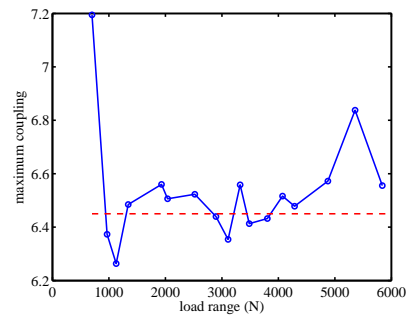
(a) Veering Parameter Datum



(b) Mean Eigenvalue at Datum



(c) Minimum Eigenvalue Separation



(d) Maximum Modal Coupling

Figure 7. Veering properties extracted from the experimental data using data points from varying load ranges, centered approximately about the veering datum. (Modes 5 and 6.)

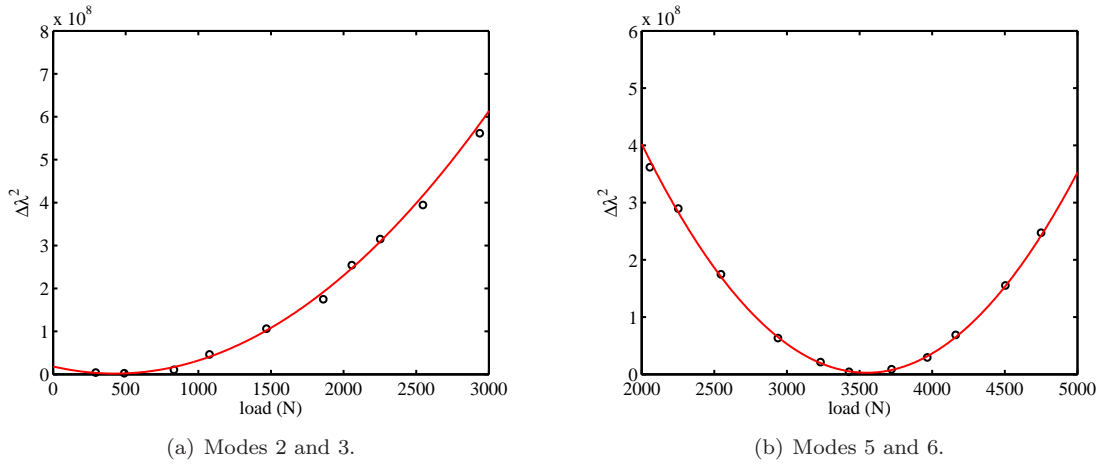


Figure 8. The quadratic curves produced with the chosen veering property values (—) compared to the measured values (○).

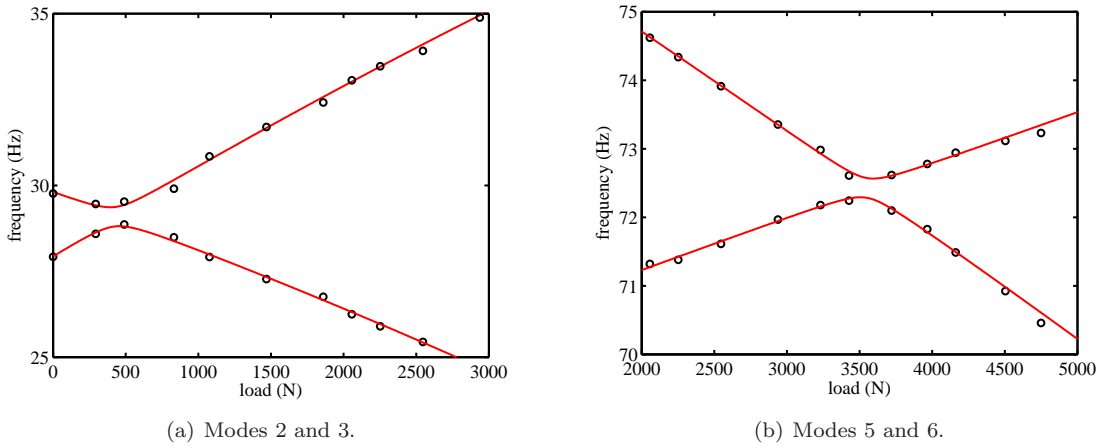


Figure 9. The eigenfrequency loci produced by the mathematical veering model (—) compared to the experimental frequency loci (○).

The chosen values produce the quadratic curves in fig. 8, corresponding with the eigenfrequency loci in fig. 9. For the purposes of the updating discussion these are taken to be accurate representations.

It has been recognised that the welds do not form perfectly rigid joints, so for the update the average joint stiffness is initialised to 70% of the full beam width. The symmetric joint differences are initialised to zero, and the Young’s modulus factor to 1. The model updating process is robust on account of the well-conditioned sensitivity matrix, and the parameter convergence is seen in Fig. 10(a) along with the updating variables. As expected for equal numbers of parameters and variables, the variables converge exactly. The parameter values obtained suggest that the joint stiffnesses are on average stiffer on the bottom of the frame and the left of the frame. The global Young’s modulus is reduced by 0.8% in the update, suggesting that the unmodelled joints are also responsible for reductions in the overall stiffness. Unfortunately for this example it is difficult to confirm these results, as inspection of the welds in the experimental rig is inconclusive. The success of this part of the exercise lies in the demonstration of a stable convergence to a unique solution.

To conclude, the results from the full nonlinear FE model are compared to the experimental data using the parameters obtained from the updating process. In Fig. 11 the veering of modes 5 and 6 is seen to be reproduced very well. Both the strength of the modal interaction and its location in the load-frequency plane are in agreement.

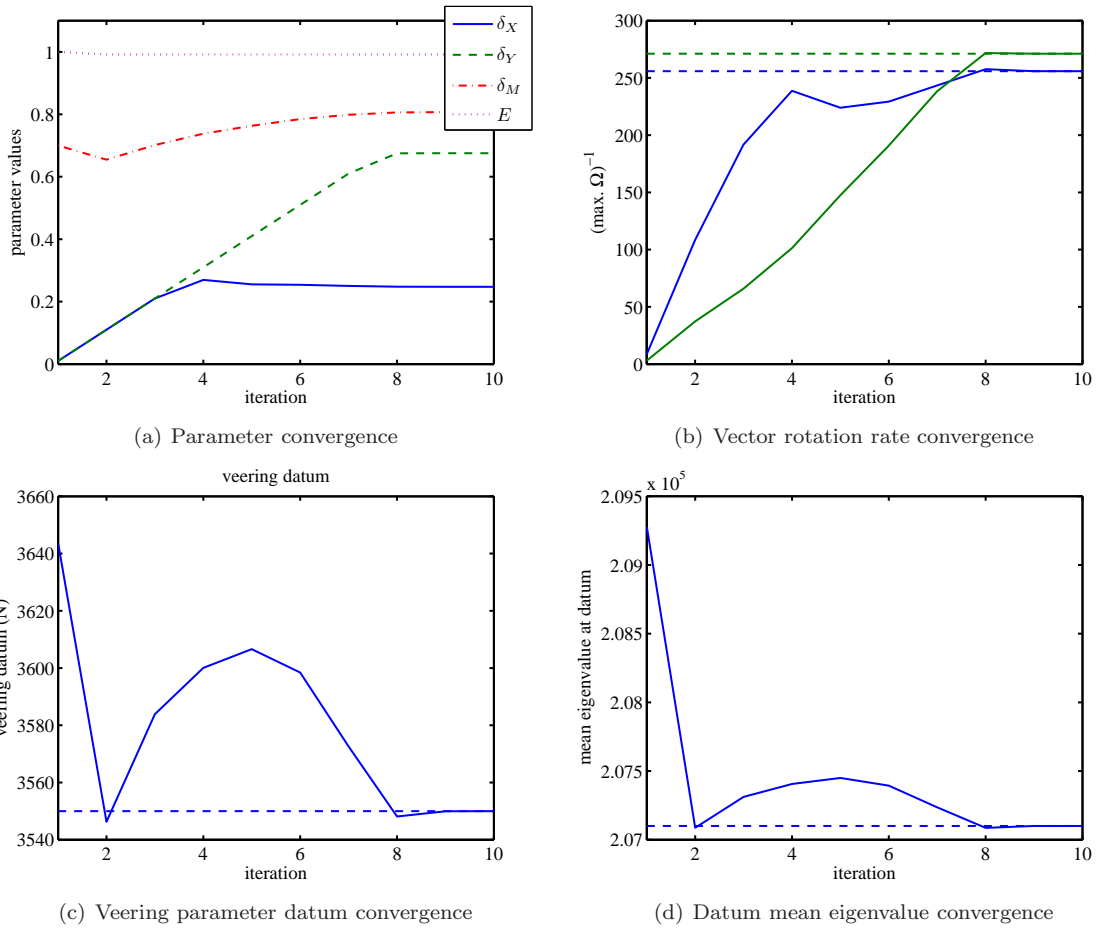


Figure 10. Parameter values and convergence history. Dotted lines indicate experimentally obtained values.

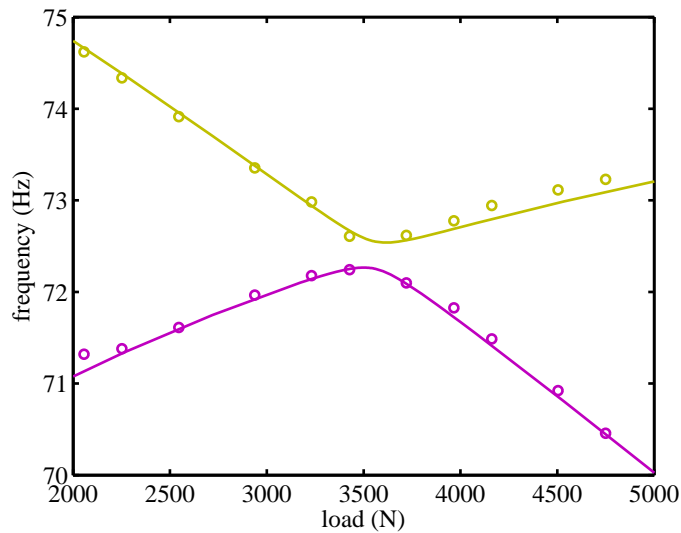


Figure 11. The eigenfrequencies of the updated FE model (—) compared to those of the experimental data (○).

VI. Discussion

The analysis above has explored the many facets of the new updating methods. In doing so it has uncovered both the strengths and weaknesses of the techniques, and highlighted key areas for further research.

Firstly, this approach is clearly capable of resolving parameter values in symmetric systems. It does so using quantitative information derived only from the eigenvalues, with the necessary extra information provided by qualitative eigenvector observations. Determining symmetric properties without this technique would involve the use of quantitative information from either the eigenvectors⁸ or the antiresonances.¹⁴ These measurements are less reliable than eigenvalue measurements as they rely on the accuracy of data from each of the measurement locations independently, and assume that the calibration of all the transducers is correct. In contrast, eigenvalue data is averaged over all the locations and does not rely on the calibration of any of the transducers. A further advantage lies in the number of measurements required: this method needs only enough measurement locations to determine the vector rotation direction. In theory two carefully selected points are enough, although in practice it is wise to incorporate redundancy by using more points.

Having claimed greater accuracy with this technique, however, it must now be acknowledged that significant uncertainties lie in the extraction of the coupling properties from the experimental data in the example above. The blame for this is attributed not to the eigenvalue measurements, but to the load measurements. This assertion raises an interesting point: the method explicitly introduces another source of measurement uncertainty with the control parameter. Thus an important consideration when devising a test strategy is to employ a control parameter that can be measured at least as accurately as the eigenvalues (in terms of the sensitivities of the coupling properties to measurement tolerances).

Other suggestions for improving the results can be made based on the choice of control parameter values. These should be limited to the region where the mass or stiffness variation obeys linear assumptions, and they should be evenly distributed either side of the veering region. The more data points that can be recorded the better the averaged results will be.

Prominent directions for new research involve firstly demonstrating the principle on a rig where the symmetric perturbations are known and the accuracy of their identification can be assessed. Using the experience gained in this study the experiment should be designed to take full advantage of the accuracy potentially afforded by this method. A direct comparison should then be made with the results of other techniques on the same rig.

Beyond the immediate development of the technique, its capabilities are thought to be relevant in a wide range of fields. Notably, localisation caused by imperfections in symmetric structures may lead to exceptionally high vibration levels, for example in turbine rotors.¹⁵ This can have severe repercussions¹⁶ and the identification of the source of localisation may help mitigate such problems. In a more abstract application, modal coupling can provide indicators of stability margins, for example in rotor blade flutter analyses.¹⁷ Accurate identification of model parameters in this case should provide powerful analytic capability. Another arena where accurate system identification is critical is in structural health monitoring; for example, frequency veering and mode “hybridisation” has recently been proposed as a method for damage monitoring in symmetric bridges.¹⁸ The scope of the updating technique is vast, with the theory upon which it is based encompassing a wide range of symmetric and periodic structures¹³ spanning many engineering disciplines.

VII. Conclusions

Although in its infancy, the technique described here has demonstrated its capability of producing a unique solution to a symmetric model updating problem. It does so using quantitative information from only the eigenvalues, giving it an advantage over techniques requiring the less reliable measurements of antiresonances and eigenvectors. The experimental exposition provided here has shown both the strengths and weaknesses of the technique; in particular an unwise choice of control parameter may introduce further inaccuracies to the results. Careful test planning is necessary to induce the eigenvalue curve veering effects upon which the

method relies, and to capture the relevant features. The results presented here show promise and some areas that may benefit from these developments include stability studies, damage detection, and localisation, in a variety of applications from turbomachinery to bridges and beyond.

Acknowledgments

Thanks are due to the EPSRC and AgustaWestland for supporting this research through research grants and a CASE award.

References

- ¹du Bois, J. L., Adhikari, S., and Lieven, N. A. J., "Experimental and Numerical Investigation of Mode Veering in a Stressed Structure," *Proceedings of the 25th International Modal Analysis Conference*, Vol. XXV, 2007, p. 233.
- ²du Bois, J. L., Adhikari, S., and Lieven, N. A. J., "Eigenvalue Curve Veering in Stressed Structures: An Experimental Study," *Journal of Sound and Vibration*, 2009, published online, doi:10.1016/j.jsv.2008.12.014.
- ³Hodges, C. H. and Woodhouse, J., "Vibration Isolation from Irregularity in a Nearly Periodic Structure: Theory and Measurements," *Journal of the Acoustical Society of America*, Vol. 74, No. 3, 1983, pp. 894–905.
- ⁴Perkins, N. C. and Mote, Jr., C. D., "Comments on Curve Veering in Eigenvalue Problems," *Journal of Sound and Vibration*, Vol. 106, No. 3, 1986, pp. 451–463.
- ⁵Balmès, E., "High Modal Density, Curve Veering, Localization: A Different Perspective on the Structural Response," *Journal of Sound and Vibration*, Vol. 161, No. 2, 1993, pp. 358–363.
- ⁶du Bois, J. L., Lieven, N. A. J., and Adhikari, S., "Localisation and Curve Veering: A Different Perspective on Modal Interactions," *Proceedings of the 27th International Modal Analysis Conference*, 2009.
- ⁷du Bois, J. L., Lieven, N. A. J., and Adhikari, S., "On the Role of Modal Coupling in Model Updating," *Proceedings of the 27th International Modal Analysis Conference*, 2009.
- ⁸Friswell, M. I. and Mottershead, J. E., *Finite Element Model Updating in Structural Dynamics*, Kluwer Academic Publishers, 1995.
- ⁹du Bois, J. L., Lieven, N. A. J., and Adhikari, S., "A New Approach to Model Updating in Symmetric Structures," *Proceedings of the 50th AIAA/ASME/ASCE/AHS/ASC Structures, Structural Dynamics, and Materials Conference*, 2009.
- ¹⁰Nelson, R. B., "Simplified Calculation of Eigenvector Derivatives," *AIAA Journal*, Vol. 14, No. 9, 1976, pp. 1201–1205.
- ¹¹Fox, R. L. and Kapoor, M. P., "Rates of Change of Eigenvalues and Eigenvectors," *AIAA Journal*, Vol. 6, No. 12, 1968, pp. 2426–2429.
- ¹²du Bois, J. L., Adhikari, S., and Lieven, N. A. J., "Experimental and Numerical Investigation of Mode Veering in a Stressed Structure," *Proceedings of the IMAC*, Vol. XXV, 2007, pp. 233.
- ¹³Bendiksen, O., "Localization phenomena in structural dynamics," *Chaos, Solitons and Fractals*, Vol. 11, No. 10, 2000, pp. 1621–1660.
- ¹⁴D'ambrogio, W. and Fregolent, A., "The use of antiresonances for robust model updating," *Journal of sound and vibration*, Vol. 236, No. 2, 2000, pp. 227–243.
- ¹⁵Ewins, D., "The effects of detuning upon the forced vibrations of bladed disks," *Journal of Sound and Vibration*, Vol. 9, No. 1, 1969, pp. 65–65.
- ¹⁶Petrov, E. and Ewins, D., "Analysis of the Worst Mistuning Patterns in Bladed Disk Assemblies," *Journal of Turbomachinery*, Vol. 125, 2003, pp. 623.
- ¹⁷Afolabi, D. and Mehmed, O., "On Curve Veering and Flutter of Rotating Blades," *Journal of Engineering for Gas Turbines and Power*, Vol. 116, 1994, pp. 702–708.
- ¹⁸Benedettini, F., Zulli, D., and Alaggio, R., "Frequency-Veering and Mode Hybridization in Arch Bridges," *Proceedings of the 27th International Modal Analysis Conference*, 2009.